18

Hydrodynamic Behavior of Flow in a Drinking Water Treatment Clarifier

Wen-Jie Yang[1], Syuan-Jhih Wu[2], Yu-Hsuan Li[2], Hung-Chi Liao[1], Chia-Yi Yang[2], Keng-Lin Shih[2] and Rome-Ming Wu[3a,b*]

[1]graduate student, Department of Chemical and Materials Engineering,
[2]undergraduate student, Department of Chemical and Materials Engineering,
*[3a]*associate professor, Department of Chemical and Materials Engineering,*
[3b]Energy and Opto-Electronic Materials Research Center,
Tamkang University, Tamsui, Taipei County,
Taiwan

1. Introduction

Over 50% drinking water was supplied to the Taiwan's public by sludge blanket clarifiers (Chen *et al*., 2003; Lin *et al*., 2004). The sludge blanket performs dual functions as a filter as well as a particle coagulator. Coagulation, the chemistry-based treatment stage, controls the characteristics of the generated sludge layer, whereas sedimentation, the hydrodynamic treatment stage, controls sludge layer stability. The existence of a sludge blanket in clarifiers is thereby essential to produce quality effluent water. In addition, the flow dynamics is an important parameter for the design of clarifiers.

The use of solids flux theory continues in many studies in the design and operation of sludge treatment processes (Takacs *et al*., 1991; Daigger, 1995; Wett, 2002). Ekama and Marais (2004) gave a survey on the development of one dimensional (1D) settler modeling. Although application of solids flux theory is good for studying the performance of clarifiers, it does not adequately describe the effect of hydrodynamic behavior in clarifiers (Narayanan *et al*., 2000). Computational fluid dynamics (CFD) has shown to be a powerful tool for resolving complex practical problems in engineering. (Hsu et al., 2007; Videla et al., 2008; Lin et al., 2008; Tao et al., 2008; Yang et al., 2007) Therefore some studies attempted to simulate full clarifiers via CFD (Deininger *et al*., 1998; Burger *et al*., 2005; Fan et al., 2007). Recently Wu *et al*. (2007) simulated flow pattern in a clarifier with porous medium as sludge blanket by 3D CFD. The first work to utilize a 3D, multiphase flow simulation for a clarifier is by Wu *et al*. (2008). Weiss *et al*. (2007) utilized non-Newtonian flow to model a circular secondary clarifier and showed that viscosity of sludge dominates the flow in clarifier. This study attempts to improve clarifier effluent quality by altering its geometric construction. The simulation is based on the sludge blanket clarifier at the Bansin Water Treatment Plant, Taiwan.

Bansin Water Treatment Plant (BWTP) is in Banchiao City, Taipei County, Taiwan. About every 20 minutes sludge blanket overturns somewhere and effluent solid flux increases. The turbidity of the clarified water is generally too high to produce quality clean water after

Source: Computational Fluid Dynamics, Book edited by: Hyoung Woo OH,
ISBN 978-953-7619-59-6, pp. 420, January 2010, INTECH, Croatia, downloaded from SCIYO.COM

sand filtering. In this work, four types of constructions of clarifiers are simulated by 3D, multiphase flow model to improve clarifier effluent quality. *Type A* is the conventional clarifier used in BWTP. *Type B* changes inlet pipe to a large one (1.6 folds). *Type C* changes reaction well angle from 120^0 to 90^0. *Type D* changes reaction well angle from 120^0 to 60^0. As shown in previous research (Yang *et al.*, 2008) that, the velocity of suspension in the reaction well is one of the factors affecting the quality of water discharge, so the improved method of *Type B* is expected to slow the velocity of flow by enlarging diameter of inlet pipe. The improvement method of *Type C* is the angle of 90^0 of reaction cover. It is hoped that the backflow could be limited within the reaction well, so that the residence time of suspension in the reaction well can be increased. The improved method for *Type D* reverses the whole reaction cover, so the water quality may not deteriorate for reason of easy outflow of the suspension from the reaction well.

2. Geometry and meshes

Figure 1 indicates the geometry of the sludge blanket clarifier. The clarifier is 19×19×5.5 m^3, with an impeller with 16 blades and diameter of 3 m. The impeller is located in center top of the clarifier. The inlet pipe is 0.9 m in diameter. The inlet pipe is connected to a draft tube 2.4 m in diameter. The inlet water velocity was typically operated at 0.34 m/s. The draft tube comprises the first reaction zone. The second reaction zone is outside the first reaction zone and inside a reaction well with upper and lower diameters of 8 and 13 m, respectively. The reaction well is 3.8 m high. Figure 2 shows all grids in the clarifier.

3. Governing equations and boundary conditions

3.1 Conservation equations.

Volume fractions represent the space occupied by each phase, and the laws of conservation of mass and momentum are satisfied by each phase individually. The volume of phase q, V_q , is defined by

$$V_q = \int_V \alpha_q dV \tag{1}$$

where α is phase volume fraction occupied by each phase, and

$$\sum_{q=1}^{n} \alpha_q = 1 \tag{2}$$

The effective density of phase q is

$$\hat{\rho}_q = \alpha_q \rho_q \tag{3}$$

where ρ_q is the physical density of phase q. In this work, only water and solid phases are considered.

The continuity equation for phase q is

$$\frac{\partial}{\partial t}(\alpha_q \rho_q) + \nabla \bullet (\alpha_q \rho_q \vec{v}_q) = \sum_{p=1}^{n} (\dot{m}_{pq} - \dot{m}_{qp}) \tag{4}$$

where $\vec{v}_q$ is the velocity of phase q and $\dot{m}_{pq}$ characterizes the mass transfer from the p to q phase, and $\dot{m}_{qp}$ characterizes the mass transfer from phase q to phase p, hence $\dot{m}_{pq} = -\dot{m}_{qp}$ and $\dot{m}_{pp} = 0$.
The momentum balance for water phase w yields

$$\frac{\partial}{\partial t}(\alpha_w \rho_w \vec{v}_w) + \nabla \bullet (\alpha_w \rho_w \vec{v}_w \vec{v}_w) = -\alpha_w \nabla P + \nabla \bullet \overline{\overline{\tau}}_w + \alpha_w \rho_w \vec{g} + (\vec{R}_{sw} + \dot{m}_{sw} \vec{v}_{sw} - \dot{m}_{ws} \vec{v}_{ws}) \tag{5}$$

where P is the pressure shared by all phases, and $\overline{\overline{\tau}}_w$ is the water phase stress-strain tensor

$$\overline{\overline{\tau}}_w = \alpha_w \mu_w (\nabla \vec{v}_w + \nabla \vec{v}_w^T) + \alpha_w (\lambda_w - \frac{2}{3}\mu_w) \nabla \cdot \vec{v}_w \bar{\bar{I}} \tag{6}$$

Here μ_w and λ_w are the shear and bulk viscosity of water phase, $\vec{R}_{sq}$ is an interaction force between water and solid phases. $\vec{v}_{sw}$ is the interphase velocity, defined as follows. If $\dot{m}_{sw} > 0$, $\vec{v}_{sw} = \vec{v}_s$; if $\dot{m}_{sw} < 0$, $\vec{v}_{sw} = \vec{v}_w$.
The momentum balance for solid phase s yields

$$\frac{\partial}{\partial t}(\alpha_s \rho_s \vec{v}_s) + \nabla \bullet (\alpha_s \rho_s \vec{v}_s \vec{v}_s) = -\alpha_s \nabla P - \nabla p_s + \nabla \bullet \overline{\overline{\tau}}_s + \alpha_s \rho_s \vec{g} + (\vec{R}_{ws} + \dot{m}_{ws} \vec{v}_{ws} - \dot{m}_{sw} \vec{v}_{sw}) \tag{7}$$

where p_s is the solids pressure. For granular flows in the compressible regime, a solids pressure is calculated independently and used for the pressure gradient term, ∇p_s, in the granular-phase momentum equation.
The solids stress tensor contains shear and bulk viscosities arising from particle momentum exchange due to translation and collision. The collisional and kinetic parts are added to give the solids shear viscosity. The solids bulk viscosity accounts for the resistance of the granular particles to compression and expansion.

3.2 Phase interactions.

$\vec{R}_{ws}$ depends on the friction, pressure, cohesion, and other effects, and is subject to the conditions that $\vec{R}_{sw} = -\vec{R}_{ws}$ and $\vec{R}_{ww} = \vec{R}_{ss} = 0$.
FLUENT uses a simple interaction term of the following form:

$$\vec{R}_{sw} = K_{sw}(\vec{v}_s - \vec{v}_w) \tag{8}$$

where $K_{sw}(= K_{ws})$ is the interphase momentum exchange coefficient. The fluid-solid exchange coefficient K_{sw} can be written in the following general form:

$$K_{sw} = \frac{\alpha_s \rho_s f}{\tau_s} \tag{9}$$

where τ_s, the particulate relaxation time, is defined as

$$\tau_s = \frac{\rho_s d_s^2}{18\mu_w} \tag{10}$$

where d_s is the diameter of particles of phase s.

For the Syamlal-O'Brien model (1989),

$$f = \frac{C_D \mathrm{Re}_s \alpha_w}{24 v_{r,s}^2} \tag{11}$$

where the drag function and relative Reynolds number have the following forms:

$$C_D = (0.63 + \frac{4.8}{\sqrt{\mathrm{Re}_s / v_{r,s}}})^2 \tag{12}$$

$$\mathrm{Re}_s = \frac{\rho_w d_s |\vec{v}_s - \vec{v}_w|}{\mu_w} \tag{13}$$

This model is based on measurements of the terminal velocities of particles in fluidized or settling beds. $v_{r,s}$ is the terminal velocity correlation for the solid phase (Garside and Al-Dibouni, 1977):

$$v_{r,s} = 0.5\left(\alpha_w^{4.14} - 0.06\mathrm{Re}_s + \sqrt{(0.06\mathrm{Re}_s)^2 + 0.12\mathrm{Re}_s\left(2\alpha_w^{2.65} - \alpha_w^{4.14}\right) + \alpha_w^{8.28}}\right) \tag{14}$$

Lift forces act on a particle mainly due to velocity gradients in the primary-phase flow field. The lift force will be more significant for larger particles. Thus, the inclusion of lift forces is not appropriate for closely packed particles or for very small particles. When a secondary phase *p* accelerates relative to the primary phase *q*, the inertia of the primary phase mass encountered by the accelerating particles exerts a virtual mass force on the particles. The virtual mass effect is significant when the secondary pahse density is much smaller than the primary phase density. Therefore virtual mass force is not either considered in this work. In order to make the calculation simple, the acting force between water and particle is dominated by the drag force, which is shown in the $\vec{R}_{sw}$ term. The other relatively strong acting forces, such as combination between particle and particle by coagulant, can be reflected in the viscosity of solid phase.

3.3 Boundary conditions.

The boundary conditions are as follows:

$$\vec{v}_s = \vec{v}_w = \vec{V} \text{ at inlet pipe} \tag{15a}$$

$$\alpha_s = 0.005 \text{ at inlet pipe} \tag{15b}$$

$$\vec{v}_s = \vec{v}_w = 0 \text{ , at walls} \tag{15c}$$

$$P = 0, \text{ at water/air surface} \tag{15d}$$

Equation (15a) and (15b) state that the inlet suspension is moving at a constant speed and has a solid volume fraction equal to 0.005. Equation (15c) describes no slip boundary

conditions for water and solid phases. Equation (15d) describes the gauge pressure at the water surface (top of the clarifier) is zero.

The computational fluid dynamics program FLUENT 6.1 (Fluent Inc., USA) solved the governing equations, together with the associated boundary conditions, using hybrid mesh volumes generated by GAMBIT. This work uses three groups of meshes of different quantities (1 million, 2 million, 2.5 million) for calculation. The relative error of the solid volume fraction at the overflow is smaller than 10%. Therefore the numbers of mesh volumes in the whole clarifier are used about 2,500,000. The calculations were carried out with maximum relative error of 10^{-4} in fluid velocity evaluation.

4. Results and discussion

4.1 Velocity vector of water flow.

Figure 3 plots the velocity vector of water in the clarifier (inlet velocity = 0.3 m/s, impeller rotation speed = 0.3 rad/s). When inlet water is flowing into the draft tube, it is sucked to the top of the clarifier, owing to the rotating impeller. Then it goes down along the inside of the well and separates into two streams. One stream inside the well makes a strong cycling flow (#1) in the secondary reaction well, the other stream rises along the wall of the clarifier, to water surface, and descends along the outside of the reaction well, making another weaker cycling flow (#2). Although this cycling flow (#2) is weaker than (#1), it is still a strong density current that the flocs will be elutriated, leading to an average 20 minutes overturn as reported in Chen *et al.* (2003). An idea is to treat the flocs into a strong and dense blanket.

5. Comparison with Bansin Water Treatment Plant (BWTP)

Bansin Water Treatment Plant (BWTP) adopted 16 sludge blanket clarifiers to treat its raw water. This type of clarifier is used by many regions to produce drinking water, but relevant references are very few. Figure 4 is a comparison between observation in BWTP and CFD results. An observer stood beside the clarifier, recorded which areas sludge blanket was floating. Thus in figures 4(a)-(d), blue color means that water surface is clean; while yellow color indicates that sludge suspension was on that surface. Figures 4(a)-(d) were the observation results at 0 s, 600 s, 900 s, and 1200 s. Figures 4(e)-(h) were volume fraction contours calculated by FLUENT at 2400 s, 3000 s, 3300 s, and 3600 s. The patterns are similar between BWTP observation and numerical calculation and that sludge overturns from edge and corner every 20 minutes. Circular clarifier might be a solution to solve this problem.

5.1 Twophase flow.

Figure 5 reveals the contour of volume fraction of solid phase of Eulerian two phase flow as time evolves. The primary phase is water phase, the secondary phase is solid phase with particle size 10 μm and density 1,005 kg/m^3. As time goes by, the solid particles were sucked from the draft tube to the top of the impeller, descends along the reaction well inside, be full of the whole reaction well, and overflow to the reaction well outside, making a relatively stable blanket at the bottom of the clarifier, and a dynamic upward particles' surface. Compared with figures 5a to 5c, it is obviously shown that as time passes, the

particles boundary becomes higher (white dash line), i.e., many particles rise and the loading of the following fast filtration becomes heavy.

In order to enunciate the geometric effects on the stability of the sludge blanket, the other three types (*Type B*, *Type C*, and *Type D*) of constructions of clarifiers were studied. Comparing with these figures it is shown that after 3600s' operation, the lowest particle concentration at the effluent surface happens at the *Type B* construction, the large inlet pipe.

As shown in Figure 6a, the increase of the caliber size of inlet pipes decelerate the fluid, thus, the intensity of backflow formed is smaller than the original structure (Fig. 3). The flow-up velocity outside of the reaction well is relatively small, and the volume fraction of particles carried upward by fluids is small as well. Finally, the quality of water discharge is favorable.

As shown in Figure 6b, the angle of the reaction well is a right angle, which is equivalent to an impinge flow when the suspension flows downward along the inside of the reaction well and approaches the bottom of the clarifier. The effective backflow cannot be formed, thus, the particles are prone to flow out of the reaction well to raise the concentration. In Figure 6c, it is expected that the suspension will be surrounded by the reversed reaction cover, thus preventing the particles from flowing out of the reaction well. However, a backflow zone is produced at the top of reaction well (as compared to the backflow zone appeared in the middle section of the reaction well in the original structure, Fig. 3). The upper backflow field at this position will hamper the backflow of the suspension under the reaction well so that it does not backflow into the reaction well, but leaving the reaction well. Thus, the concentration of the suspension outside the reaction well is raised.

Effluent upflow velocity (EUV) is proposed as an important parameter affecting clarifier performance (Narayanan *et al*., 2000). In this simulation work, effluent solid flux can be calculated in advance. The effluent solid flux is displayed in figure 7. For *Type A* and *Type B*, effluent solid flux increase steadily; while for *Type C* and *Type D*, effluent solid flux increase saw-toothed. This might due to the squeezed backflow in top of the reaction well causing unstable flow field outside the reaction well. Before 2500s, effluent solid flux is less than 0.05 kg/m^2-s except for *Type D*. After 2500s, effluent solid flux is increasing dramatically. It is suggested that BWTP could drain sludge away per hour according to this simulation work. At almost all the 3000s' operations, the effluent solid flux is the lowest in *Type B* construction.

6. Conclusions

Blanket floc volumetric concentration is an important parameter in understanding the performance of sludge blanket clarifiers. 3D simulations of a clarifier using four different geometric constructions were studied in this work. From the simulation results of effluent solid flux, it is suggested that under the same daily throughput the large inlet pipe can reduce the flow velocity in the clarifier, hence reduce effluent solid flux and improve the quality of water. According to this simulation results, it is recommended that BWTP has to make large inlet pipe to obtain good quality water under the same daily throughput, or obtain large daily throughput under the same quality water.

The simulation results can only be interpreted qualitatively and not quantitatively since only hydrodynamic behavior is considered. Further work should concern the chemical

based treatment, i.e., coagulation of flocs in clarifier. Nevertheless, the simulation results can show tendencies in the flow pattern due to changes in clarifier construction.

7. Acknowledgment

The authors would like to thank the National Science Council of the Republic of China, Taiwan, for financially supporting this research under Contract No. NSC 96-2221-032-020.

8. References

Burger, R., K. H. Karlsen, and J. D. Towers, "Mathematical Model and Numerical Simulation of the Dynamics of Flocculated Suspensions in Clarifier-Thickeners," *Chem. Eng. J.*, 111, 119 (2005).

Chen, L. C., S. S. Sung, W. W. Lin, D. J. Lee, C. Huang, R. S. Juang, and H. L. Chang, "Observations of Blanket Characteristics in Full-Scale Floc Blanket Clarifiers," *Water Sci. and Tech.*, 47, 197 (2003).

Daigger, D. T. "Development of Refined Clarifier Operating Diagrams using An Updated Settling Characteristics Database," *Water Environ. Res.*, 67, 95 (1995).

Deininger, A.,E. Holthausen, and P. A. Wilderer, "Velocity and Solids Distribution in Circular Secondary Clarifiers: Full Scale Measurements and Numerical Modeling," *Water Res.*, 32, 2951 (1998).

Ekama, G. A. and P. Marais, "Assessing the Applicability of the 1D Flux Theory to Full-Scale Secondary Settling Tank Design with a 2D Hydrodynamic Model," *Water Res.*, 38, 495 (2004).

Fan, L., N. Xu, X. Ke, and H. Shi, "Numerical Simulation of Secondary Sedimentation Tank for Urban Wastewater," *J. Chin. Inst. Chem. Eng.*, 38, 425 (2007).

Garside, J. and M. R. Al-Dibouni, "Velocity-Voidage Relationships for Fluidization and Sedimentation," *Ind. Eng. Chem. Process Design and Develop.*, 16, 206 (1977).

Hsu, J. P., S. C. Yang, and J. C. Chen, "Drag on Two Co-axial Rigid Spheres Moving Normal to A Plane: Newtonian and Carreau Fluids," *J. Chin. Inst. Chem. Eng.*, 38, 409 (2007).

Lin, W. W., S. S. Sung, L. C. Chen, H. Y. Chung, C. C. Wang, R. M. Wu, D. J. Lee, C. Huang, R. S. Juang, X. F. Peng, and H. L. Chang, "Treating High-Turbidity Water Using Full-Scale Floc Blanket Clarifiers," *J. Environ. Eng.-ASCE*, 130, 1481 (2004).

Lin, J. S., C. J. Tsai, K. L. Tung, H. C. Chiang, "Thermophoretic Particle Deposition Efficiency in Turbulent Tube Flow," *J. Chin. Inst. Chem. Eng.*, 39, 281 (2008).

Narayanan, B., S. G. Hough, and R. J. Ooten, "New Hypothesis for Secondary Clarifier Performance under Hydraulically Limited Conditions," *Water Environ. Res.*, 72, 116 (2000).

Syamlal, M. and T. J. O'Brien, "Computer Simulation of Bubbles in a Fluidized Bed," *American Institute of Chemical Engineering Symposium Series*, 85, 22 (1989).

Takacs, I., G. G. Patry, and D. Nolasco, "A Dynamic Model of the Clarification-Thickening Process," *Water Res.*, 25, 1263 (1991).

Tao, T., X. F. Peng, A. Su, D. J. Lee, "Modeling Convective Drying of Wet Cake," *J. Chin. Inst. Chem. Eng.*, 39, 287 (2008).

Videla, A. R., C. L. Lin, and J. D. Miller, "Simulation of Saturated Fluid Flow in Packed Particle Beds-The Lattice-Boltzmann Method for the Calculation of Permeability from XMT Images," *J. Chin. Inst. Chem. Eng.*, 39, 117 (2008).

Weiss, M., B. G. Plosz, K. Essemiani, and J. Meinhold, "Suction-Lift Sludge Removal and Non-Newtonian Flow Behaviour in Circular Secondary Clarifiers: Numerical Modeling and Measurements," *Chem. Eng. J.*, 132, 241 (2007).

Wett, B. "A Straight Interpretation of the Solids Flux Theory for a Three-Layer Sedimentation Model," *Water Res.*, 36, 2949 (2002).

Wu, R. M., T. H. Lee, W. J. Yang, "Study of Water Treatment Clarifier," *Tamkang J. of Sci. and Eng.*, 10, 317 (2007).

Wu, R. M., T. H. Lee, and W. J. Yang, "Study of Flow in a Blanket Clarifier Using Computational Fluid Dynamics," *J. Environ. Eng.-ASCE*, 134, 443 (2008).

Yang, W. J., C. C. Wang, R. Y. Hsu, and R. M. Wu, "Two-Phase Flow Simulation of Reactor Clarifiers," *J. Chin. Inst. Chem. Eng.*, 39, 275 (2008).

Yang, Z., X. F. Peng, D. J. Lee, and A. Su, "Reynolds Number-Dependent Permeability of Wastewater Sludge Flocs," *J. Chin. Inst. Chem. Eng.*, 38, 135 (2007).

9. Nomenclature

C_D	drag coefficient, -
K	interphase momentum exchange coefficient, -
d_s	diameter of particle, m
f	correlation factor, -
$\vec{g}$	acceleration of gravity, m/s^2
$\dot{m}_{pq}$	mass transfer from p to q phase, kg/m^3-s
P	pressure, N/m^2
p_s	solid pressure, N/m^2
Re_s	Reynols number, -
$\vec{R}$	water/solid interaction, N/m^2
V	volume of each phase, m^3
$v_{r,s}$	terminal velocity correlation, -
$\vec{v}$	water/solid velocity, m/s
α	volume fraction, -
μ	shear viscosity, kg/m-s
λ	bulk viscosity, kg/m-s
ρ	density, kg/m^3
$\hat{\rho}$	effective density, kg/m^3
τ_S	particulate relaxation time, s
$\bar{\bar{\tau}}$	stress tensor, N/m^2

Subscripts

w	water phase
s	solid phase

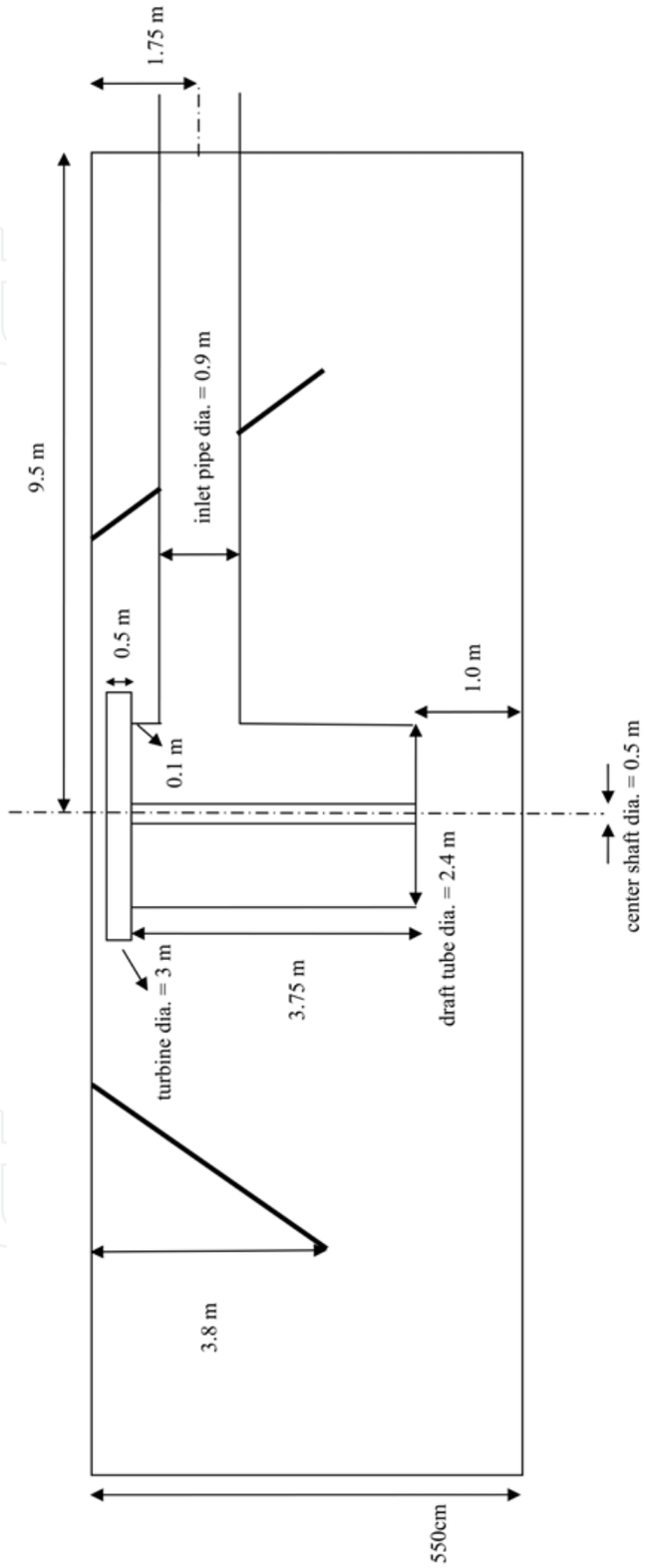

Fig. 1. Geometry of the clarifier

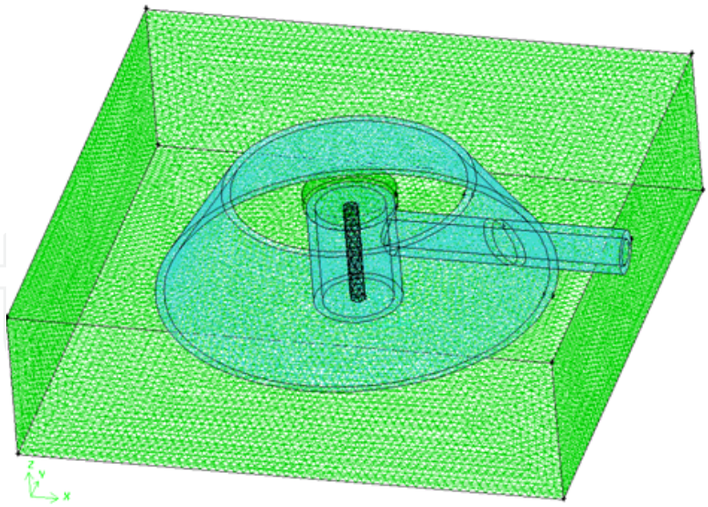

(a)

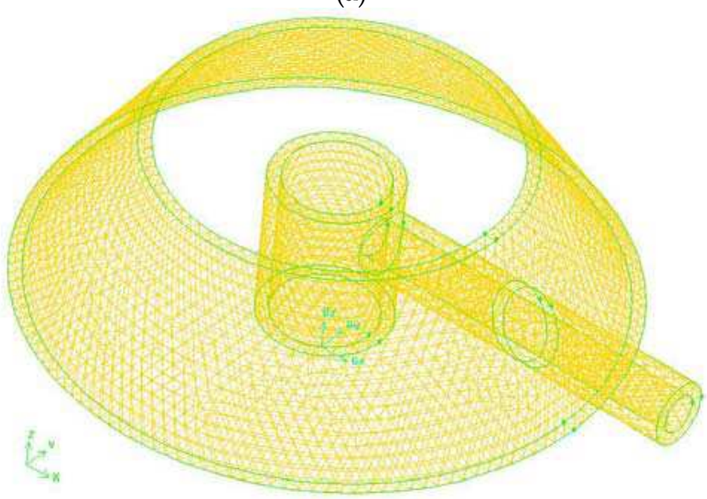

(b)

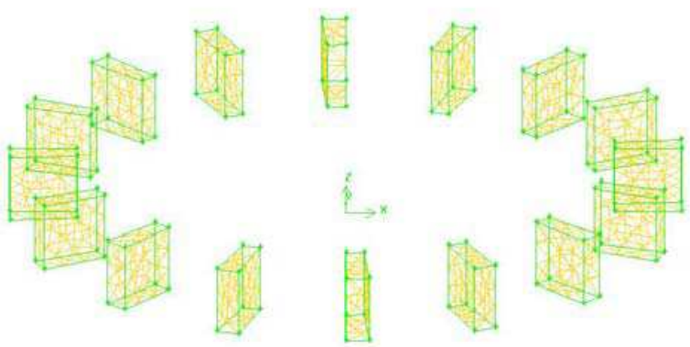

(c)

Fig. 2. Meshes of the clarifier (a) whole clarifier (b) reaction well, inlet pipe, and draft tube (c) blades

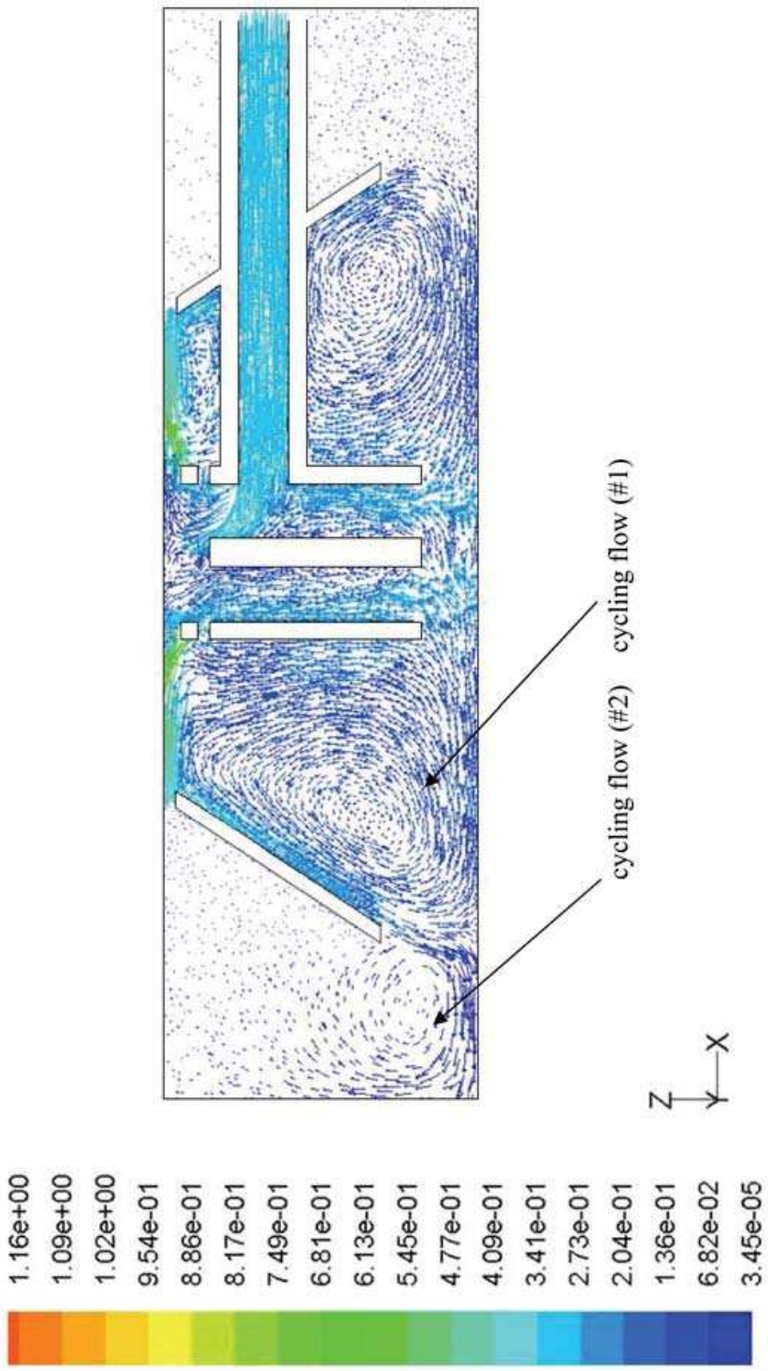

Fig. 3. Velocity vector of water flows (inlet velocity = 0.3 m/s, impeller rotation speed = 0.3 rad/s)

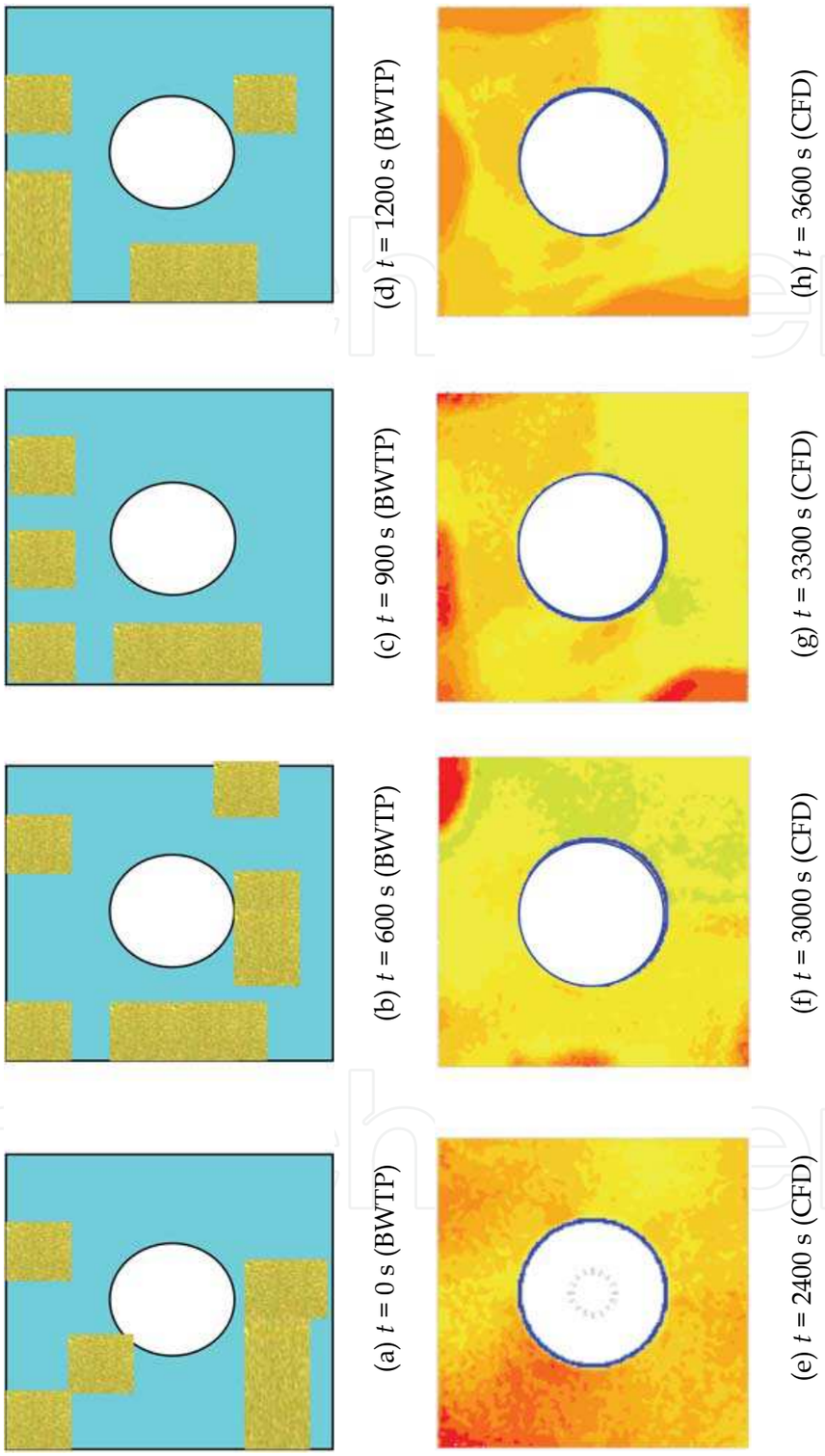

Fig. 4. Contour of solid volume fraction on water surface (a) t = 0 s (BWTP) (b) t = 600 s (BWTP) (c) t = 900 s (BWTP) (d) t = 1200 s (BWTP) (e) t = 2400 s (CFD) (f) t = 3000 s (CFD) (g) t = 3300 s (CFD) (h) t = 3600 s (CFD)

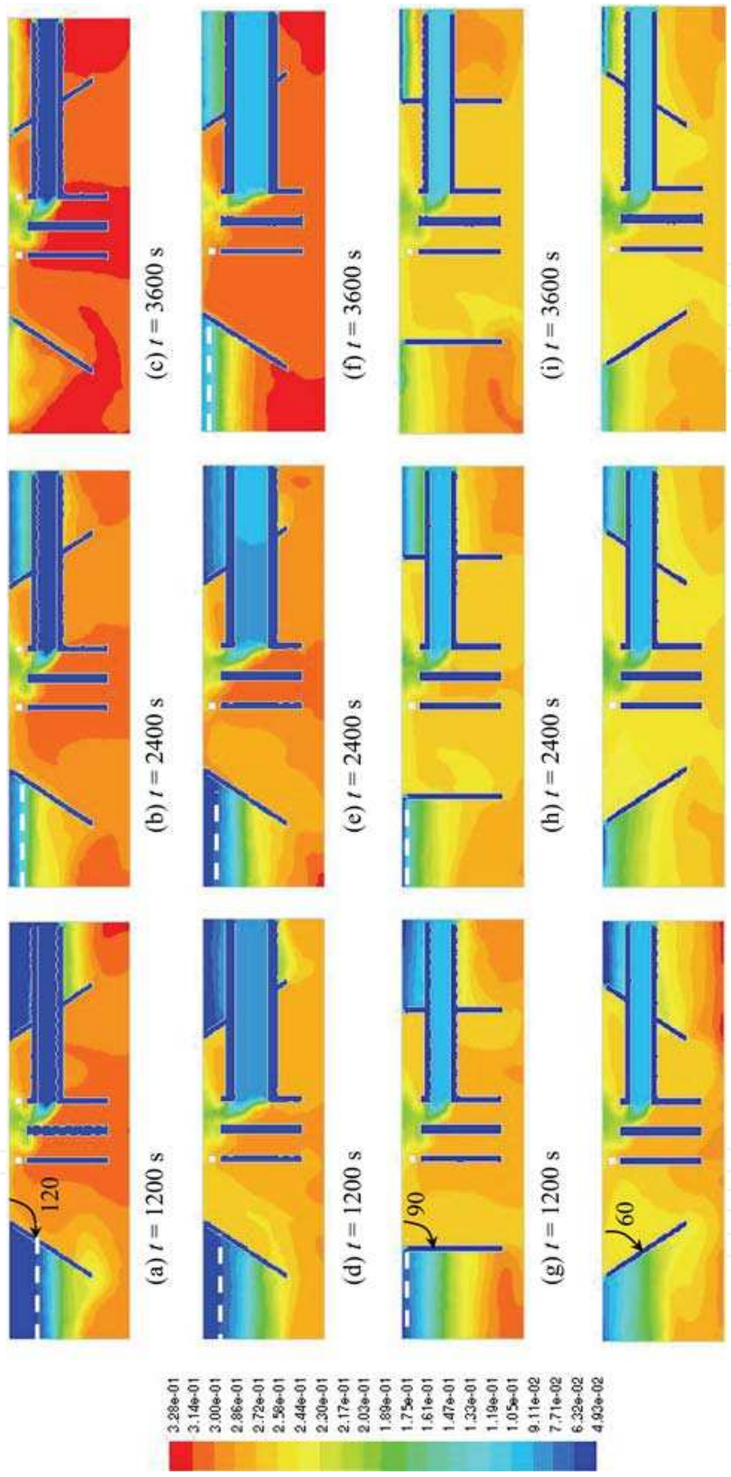

Fig. 5. Contour of solid volume fraction in clarifier (a) *Type A*, *t* = 1200 s (b) *Type A*, *t* = 2400 s (c) *Type A*, *t* = 3600 s (d) *Type B*, *t* = 1200 s (e) *Type B*, *t* = 2400 s (f) *Type B*, *t* = 3600 s (g) *Type C*, *t* = 1200 s (h) *Type C*, *t* = 2400 s (i) *Type C*, *t* = 3600 s (j) *Type D*, *t* = 1200 s (k) *Type D*, *t* = 2400 s (l) *Type D*, *t* = 3600 s

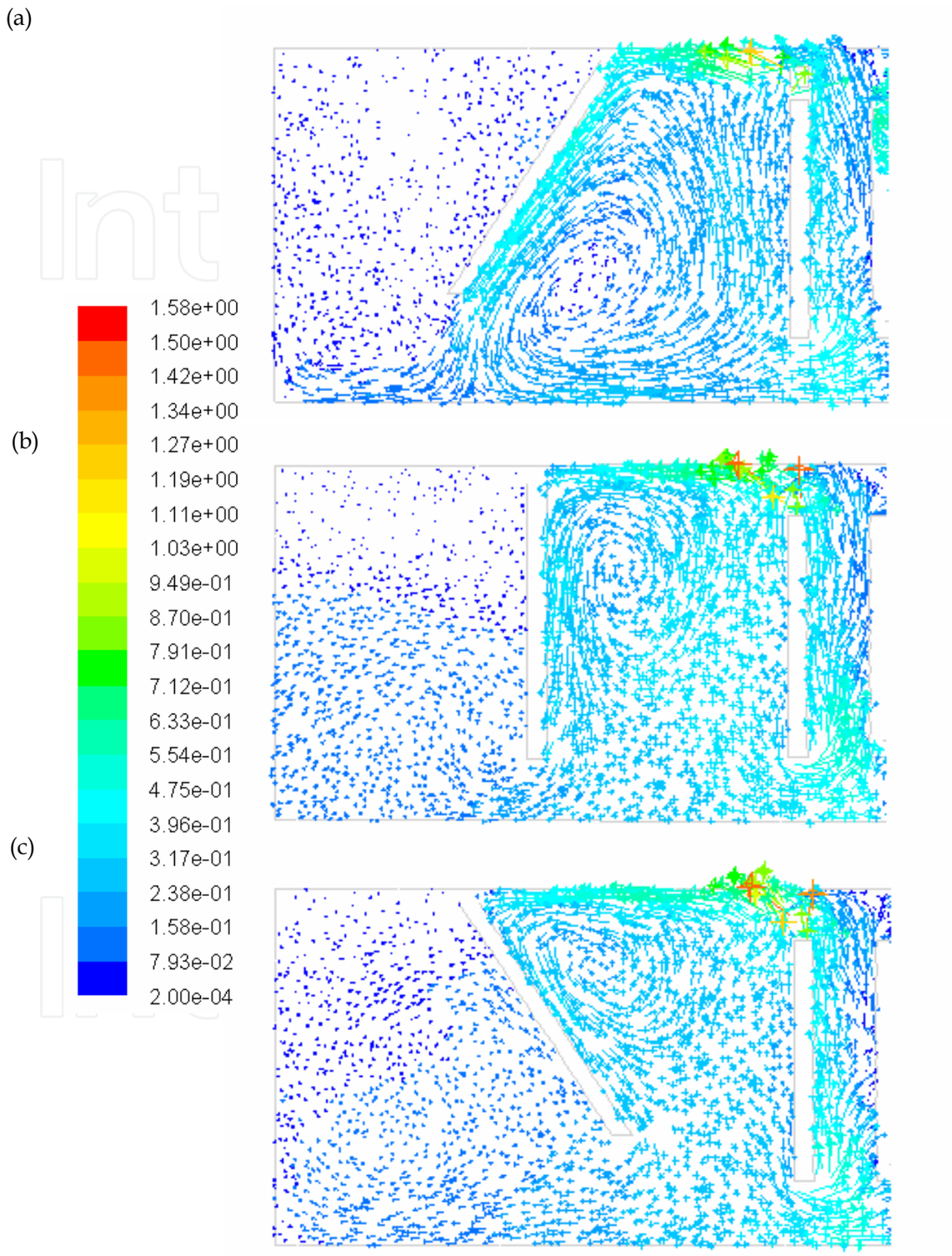

Fig. 6. Velocity vector of water flows (inlet velocity = 0.3 m/s, impeller rotation speed ω = 0.3 rad/s). (a) *Type B* (b) *Type C* (c) *Type D*

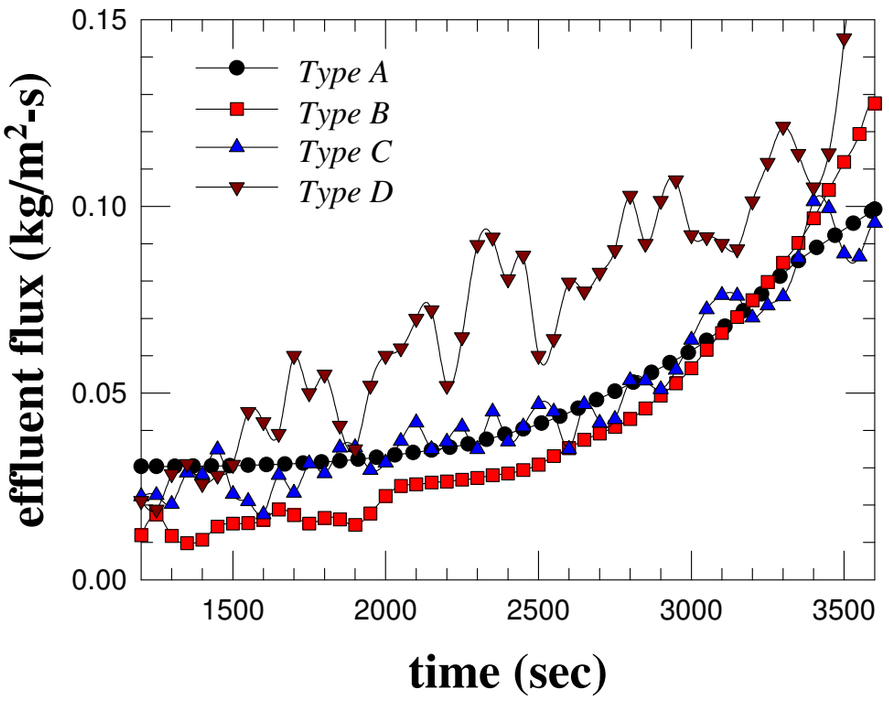

Fig. 7. Effluent solid flux of four constructions of clarifiers

Computational Fluid Dynamics

Edited by Hyoung Woo Oh

ISBN 978-953-7619-59-6

Hard cover, 420 pages

Publisher InTech

Published online 01, January, 2010

Published in print edition January, 2010

This book is intended to serve as a reference text for advanced scientists and research engineers to solve a variety of fluid flow problems using computational fluid dynamics (CFD). Each chapter arises from a collection of research papers and discussions contributed by the practiced experts in the field of fluid mechanics. This material has encompassed a wide range of CFD applications concerning computational scheme, turbulence modeling and its simulation, multiphase flow modeling, unsteady-flow computation, and industrial applications of CFD.

InTech Europe
University Campus STeP Ri
Slavka Krautzeka 83/A
51000 Rijeka, Croatia
Phone: +385 (51) 770 447
Fax: +385 (51) 686 166
www.intechopen.com

InTech China
Unit 405, Office Block, Hotel Equatorial Shanghai
No.65, Yan An Road (West), Shanghai, 200040, China
中国上海市延安西路65号上海国际贵都大饭店办公楼405单元
Phone: +86-21-62489820
Fax: +86-21-62489821

IntechOpen